What Forces Bind Liquid Crystals?

Brian D. Swanson* and Larry B. Sorensen
Department of Physics, University of Washington, Seattle, Washington 98195
(Received 6 September 1994)

The surface freezing transitions in four liquid crystals (9O.4, 4O.7, 7O.7 and $\overline{14}$S5) have been studied to determine the temperature dependence and the finite-size behavior of their effective interface potentials. The effective interface potentials are simply related to the attractive pair potentials between the molecules, and were used to probe the forces that bind these liquid crystals. Our measurements provide strong evidence for the two attractive forces expected theoretically in liquid crystals, long-range van der Waals and short-range exponential forces, and also admit the possibility of the recently predicted "thermal-Casimir" forces.

PACS numbers: 61.30.–v, 64.70.Md, 82.65.Dp

What attractive forces bind liquid crystals? Most of the usual forces which bind condensed matter (namely, the ionic, covalent, metallic, and hydrogen bonding forces) are absent in conventional thermotropic liquid crystals. This would appear to leave only the usual van der Waals forces to bind these liquid crystals. There are, however, two special attractive forces which might also help bind liquid crystals: (1) long-range "thermal-Casimir" forces which decay algebraically with distance, and (2) short-range effective forces which decay exponentially with distance. This Letter describes our experimental search for evidence that these two special forces help bind liquid crystals, and describes new effective forces due to finite system size.

The recently predicted [1] thermal-Casimir forces are due to the dipole-dipole interactions between the thermally fluctuating permanent dipoles of the liquid crystal molecules. The thermal-Casimir forces are the thermal analogs of the quantum mechanical van der Waals forces which are due to the dipole-dipole interactions between the quantum fluctuation induced dipole moments of the molecules. The magnitudes of the nematic- and smectic-thermal-Casimir forces in liquid crystals are predicted to be comparable to the magnitudes of the usual van der Waals forces. The smectic-thermal-Casimir forces, which should help bind smectic liquid crystals, are due to the thermally driven smectic layer fluctuations. These forces can be distinguished from the usual van der Waals forces because the effective pair potential [2] for the smectic-thermal-Casimir forces decays more slowly with distance (as r^{-5}) then the van der Waals contribution, which decays as r^{-6}.

The short-range effective force is a predicted consequence of the order parameter profile near the surfaces. The surface tension quenches the smectic layer fluctuations near the surface and thereby enhances the smectic layering near the surface [3]. This surface-enhanced smectic layering has been shown experimentally [4] to decay exponentially with distance from the surface. This exponential decay of the smectic order parameter will create an exponentially decaying short-range effective force [5].

How can the relative contributions of the van der Waals, thermal-Casimir, and exponential forces be determined experimentally for different liquid crystals? The two best experimental methods for studying the distance dependence of the intermolecular interactions in liquid crystals are layer-by-layer surface freezing measurements [6,7] and surface force apparatus measurements [8]. Both of these methods determine the sum of all of the forces versus distance, and not the individual forces. The relative contributions must be obtained by analyzing the distance dependence of the sum. Unfortunately, surface force apparatus measurements can be used only to probe the behavior of the forces in contact with a solid wall, and not at a free surface. There have been surface force apparatus measurements reported [8] for lyotropic liquid crystals that demonstrate the importance of the electrostatic interactions in charged lyotropic smectic phases, but surface force apparatus techniques have apparently no been used to study the origin of the forces in thermotropic smectic liquid crystals.

We showed previously [6,7] how the layer-by-layer surface freezing of thermotropic liquid crystals could be used to determine the distance dependence of the intermolecular forces. Our measurements for the thermotropic liquid crystal 9O.4 showed that 9O.4 is dominated by van der Waals forces. There is no evidence for any thermal-Casimir or exponential force contributions to the binding of 9O.4. One of our major motivations for the current study was to see whether the behavior we found for 9O.4 is universal: Is the binding of all thermotropic liquid crystals dominated by van der Waals forces, or are there systems where the thermal-Casimir and/or exponential forces also contribute, or even dominate? Very recently, layer-by-layer surface freezing measurements of the first-order smectic-*A* to smectic-*B* transition made using heat capacity techniques have shown that the homologous liquid crystal 4O.8 is also dominated by van der Waals forces [9]. In this Letter, we report the results of layer-by-layer surface freezing measurements for four liquid crystals [10], 9O.4, 4O.7, 7O.7, and $\overline{14}$S5.

0031-9007/95/75(18)/3293(4)$06.00

To determine the distance dependence of the intermolecular pair potential from the measured layer-by-layer surface freezing data it is very convenient to use the effective interface potential formalism [11]. The effective interface potential is given by the sum of two terms: (1) the conversion energy term A-ΔT, which is proportional to the temperature difference from the transition temperature $\Delta T = T - T_c$ and to the thickness of the surface frozen layer l; and (2) the interfacial energy term $\Delta\gamma[1 - f(l)]$, where the interfacial energy correction $\Delta\gamma f(l)$ is obtained by integrating the pair potential over the system [2,11]. For the two simplest cases, long-range power-law forces, and short-range exponential forces, the respective effective interface potentials are given by

$$V_{\mathrm{pow}}(l, \Delta T) = Al\Delta T + \Delta\gamma(1 - \lambda l^{1-n}), \quad (1)$$

$$V_{\mathrm{exp}}(l, \Delta T) = A'l\Delta T + \Delta\gamma(1 - \lambda' e^{-l/\xi}). \quad (2)$$

All conventional surface freezing theories [12] predict these same two functional forms. Here A and A' are constants specified by the chemical potential difference, and $\Delta\gamma = \gamma_{1V} - \gamma_{12} - \gamma_{2V}$ is the difference in interfacial energy.

The relationship between l and ΔT is obtained by minimizing the effective interface potential [11]. For power-law forces, minimization yields $\Delta T(l) = \alpha l^{-n}$ and the theoretical predictions are very explicit: (a) For nonretarded long-range van der Waals forces, the measured n must be consistent with $n = 3$; (b) for retarded van der Waals forces, the measured n must be consistent with $n = 4$; and (c) for thermal-Casimir forces, the measured n must be consistent with $n = 2$. For short-range exponential forces, minimization yields $\Delta T(l) = \beta \exp(-l/\xi)$, and the theoretical predictions about the allowed values of ξ are not as specific, but the characteristic range of the force should be about one layer.

The experimental apparatus has been described in detail previously [6,7]. It consists of a temperature-regulated freely suspended liquid crystal film oven mounted in a chamber filled with 300 torr of N_2. Because the tilted liquid crystal phases are birefringent, the monolayer freezing transitions could be observed optically through crossed polarizers. Video images of uniform thickness 7 mm diameter films of each liquid crystal were recorded versus the oven temperature. Typical cooling rates were 5–10 mK/min. We analyzed the video images to determine the temperature when each transition first appeared. The surface freezing transitions in all four liquid crystals appeared both on heating and on cooling, and were hysteric as expected for first-order surface freezing transitions. A careful study of 9O.4 showed that an undercooling of about 40 mK was required to produce each surface frozen layer [7].

For the four liquid crystals that we studied, the frozen surface phases were identified optically, based on the observed textures, as tilted hexatic smectic-I or smectic-F phases on a smectic-A interior [7]. Because these surface phases are not in the bulk phase diagrams of these liquid crystals, all of the surface freezing transitions that we studied correspond technically to incomplete wetting: For a semi-infinite system, the surface-stabilized phase would always have a finite, albeit very large, thickness. For example, although we observed 983 layer-by-layer surface freezing transitions for a 983 layer thick 4O.7 film corresponding to the surface freezing of the entire film, for a much thicker film there would only be a finite number of layer-by-layer surface freezing transitions on each free surface.

To determine the form of the intermolecular pair potential in the four liquid crystals, we fit the first ten surface freezing transitions in $L \sim 64$ layer thick films. Films in this thickness range could be precisely selected by their distinctive blue color. The fits and the best-fit parameters from the power-law and exponential force models are shown in Fig. 1 and Table I, respectively. From Fig. 1 and Table I, we can conclude the following. (a) The 9O.4 data set is only consistent with van der Waals forces and demonstrates that some liquid crystals are dominated by van der Waals interactions with no apparent contributions from exponential for thermal-Casimir forces. (b) The 7O.7 data set is only consistent with exponential forces; the power-law fit gives an unphysical exponent $n = 6$. (c) The 4O.7 data set is equally consistent with thermal-Casimir forces or with exponential forces. Thus 4O.7 may be a liquid

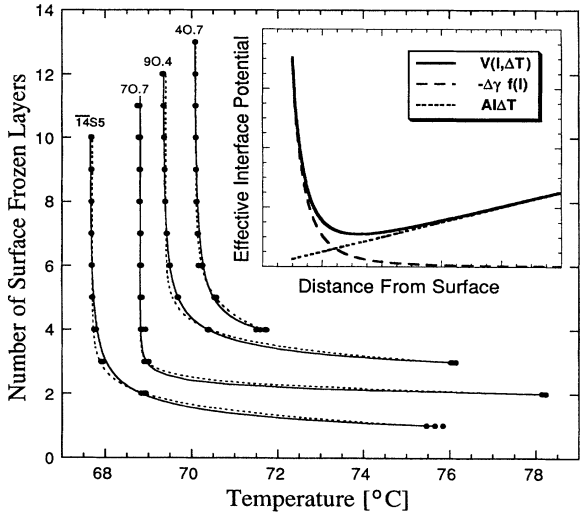

FIG. 1. The measured number of frozen surface layers versus temperature. For visual clarity, the successive liquid crystals have been shifted up by +1 layers and the 4O.7 data set has been shifted by +21 °C. The solid lines indicate the results of the fits to the long-range power-law force model, and the dashed lines indicate the results for the short-range exponential force model. Inset: The simple effective interface potential $V(l, \Delta T)$ produced by the sum of the conversion energy term $Al\Delta T$ and the interfacial energy correction $-\Delta\gamma f(l)$; the constant offset due to $\Delta\gamma$ is not shown.

TABLE I. The best-fit parameters for the long-range power-law and the short-range exponential force models. The power-law fits used $T(l) = T_c + \alpha l^{-n}$. The exponential force fits used $T(l) = T_c' + \beta e^{-l/\xi}$. For each liquid crystal, N different films were measured. The forces that fit the data for each liquid crystal are indicated by van der Waals (v), thermal-Casimir (c), and exponential (e).

LC	N	Allowed Forces	Power law T_c	α	n	Exponential T_c'	β	ξ
9O.4	6	v	69.331	6.78 ± 0.05	2.69 ± 0.03	69.397	39.1 ± 0.5	0.56 ± 0.01
4O.7	5	c,e	49.107	1.71 ± 0.01	1.98 ± 0.11	49.160	5.0 ± 0.8	0.86 ± 0.07
7O.7	3	e	69.188	9.40 ± 0.05	5.8 ± 0.8	69.191	(5.9 ± 2.3) × 10^2	0.25 ± 0.02
$\overline{14}$S5	4	v,e	67.621	8.11 ± 0.16	3.12 ± 0.06	67.687	50.1 ± 3.1	0.54 ± 0.02

crystal dominated by smectic-thermal-Casimir forces. (d) The $\overline{14}$S5 data set is equally consistent with van der Waals or exponential forces. The quality of our force determination is limited by the quality of the surface freezing data. Although the power-law and exponential force model appear to fit all four liquid crystals equally well, the errors on the 9O.4 data are much smaller than the dots [6,7], and consequently the exponential force model is not consistent with the 9O.4 data. We do not know why 9O.4 is more reproducible than the other three liquid crystals.

Beyond about the first ten surface freezing transitions, the subsequent surface freezing transitions proceed more slowly than the predicted divergence. Of course, a true divergence is predicted only in the thermodynamic limit. The observed slowdown depends on the film thickness. These finite-size slowdown effects, first noticed in 9O.4 [6], have been studied versus film thickness for 4O.7 and 7O.7 films with thicknesses ranging from 17 to ~1000 layers [7]. In all three systems, the surface freezing transitions displayed a systematic and progressive deviation from the initial power-law or logarithmic divergence. Figure 2 shows the observed slowdown versus film thickness for 4O.7. The surface freezing transitions in thicker films proceed more quickly with temperature than the transitions in thinner films.

The data set shown in Fig. 2 was fit to a phenomenological finite-size model which assumed the same short-range exponential force parameters which fit the data for the first ten layers and which predicted the surface freezing temperature for the lth layer to be $T(l) = T_c + \beta \exp(-l/\xi) - \beta' L/(L - \varepsilon l)$. Although no explicit theory exists for finite-size effects in freely suspended smectic liquid crystal films, our model corresponds to a shift in the surface freezing temperature of the lth layer $\delta T(L, l) \propto 1/(L - \varepsilon l)$, which is inversely proportional to the thickness of the intermediate "unfrozen" region of the film. Although our model is completely phenomenological, we find that a single set of parameters fits all of the measured 4O.7 films with $\beta' = 0.3$ and $\varepsilon = 1.1$. All of the 7O.7 data sets were also fitted with

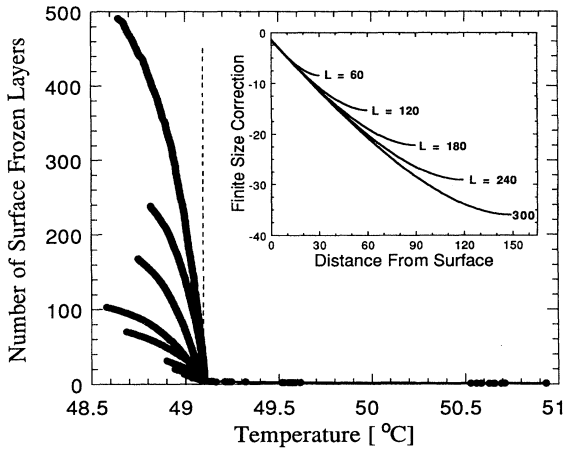

FIG. 2. The finite-size slowdown in the number of frozen surface layers versus temperature for L = 17, 27, 41, 64, 141, 207, 337, 477, and 983 layer thick 4O.7 films. The solid line through each data set (indistinguishable from the data) is the best fit to the complete effective interface potential. The dashed line indicates the predicted divergence which would occur for $V'(l; L) = 0$. Inset: The corresponding film thickness dependence of $V'(l; L)$ is shown for L = 60, 120, 180, 240, and 300 layers. Note that $V'(l; L)$ is linear in l near the surface.

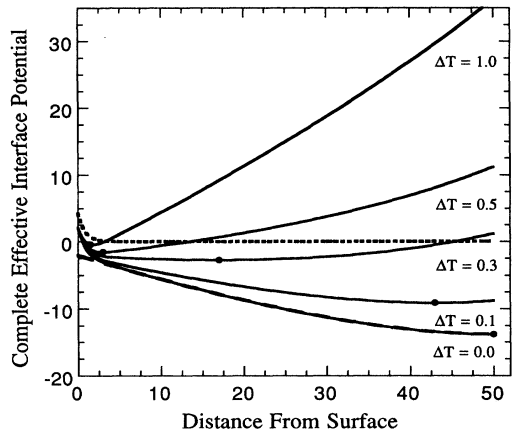

FIG. 3. The evolution of the model-independent complete effective interface potential for a 100 layer thick 4O.7 film versus temperature ($\Delta T = T - T_c$). The solid dot at the minimum of each curve indicates the number of surface frozen layers. The short-dashed line indicates the interfacial energy correction term $-\Delta\gamma f(l)$ and the long-dashed line indicates the finite-size correction term $V'(l; L)$. Note that for small l, $V'(l; L)$ simply renormalizes the temperature, but for large l it produces the finite-size slowdown.

this model with $\beta' = 0.3$ and $\varepsilon = 1.2$. The analogous finite-size model with a power-law form for the interfacial energy correction also fits the 9O.4 data [7].

The superb agreement between our phenomenological finite-size model and the data allowed us to construct the complete effective interface potential $V_c(l, \Delta T; L)$ $V(l, \Delta T) + V'(l'; L)$, by adding the finite-size correction, $V'(l; L) = -(\beta' L/\varepsilon) \ln(L - \varepsilon l)$, to the interfacial energy and conversion energy terms. Figure 3 shows the evolution of $V_c(l, \Delta T; L)$ versus temperature for a 100 layer 4O.7 film. As $\Delta T \to 0$, the minimum of V_c broadens and the position of the interface between the surface frozen phase and the unfrozen interior phase moves toward the center of the film. The "interface-interface repulsion" which slows down the transitions near the center of the film is due to $V'(l; L)$.

Figure 2 shows the thickness dependence of the finite-size correction $V'(l; L)$. For the first few transitions in films with $L > 30$ layers, $V'(l; L)$ is linear and this produces a simple shift δ of the transition temperature so that $V_c(l, \Delta T; L) \approx V(l, \Delta T + \delta)$. Although the results shown in Fig. 2 were constructed using a specific model, the complete effective interface potential is actually model independent. We have used other parametrizations of the finite-size correction and obtained indistinguishable results. In principle, of course, only the minimum of the complete effective interface potential versus temperature is determined by our measurements. However, in practice the calculated potentials were independent of our parametrization of the finite-size correction once the standard forms for $f(l)$ and $Al\Delta T$ are assumed.

To summarize, the four liquid crystals that we studied provide evidence for all three types of interactions expected for liquid crystals: van der Waals, exponential, and "thermal-Casimir" forces. This is the first report of data consistent with smectic-thermal-Casimir forces associated with the smectic layer fluctuations and the first report of data consistent with exponential forces for smectic-to-smectic transitions. The layer-by-layer surface freezing of a few smectic layers at the isotropic-vapor interface [13] is apparently also governed by exponential effective forces since the measured surface freezing transitions follow the characteristic logarithmic growth form. We also constructed the model independent complete effective interface potential and analyzed its finite-size dependence. We found that the finite-size effects produce temperature shifts inversely proportional to the size of the system. Our measurements are the only experimental studies of the different possible distance dependences of the intermolecular interactions in thermotropic smectic liquid crystals.

*Current address: Geophysics Program AK-50, University of Washington, Seattle, Washington 98195.

[1] L. V. Mikheev, Sov. Phys. JETP **69**, 358 (1988); A. Ajdari, L. Peliti, and J. Prost, Phys. Rev. Lett. **66**, 1481 (1991); Hao Li and Mehran Karder, Phys. Rev. Lett. **67**, 3275 (1991); L. V. Mikheev, Phys. Rev. Lett. **69**, 860 (1992); A. Ajdari, B. Duplantier, D. Hove, L. Peleti, and J. Prost, J. Phys. II (France) **2**, 487 (1992); M. L. Lyra, M. Kardar, and N. F. Svaiter, Phys. Rev. E **47**, 3456 (1993).

[2] As is well known for retardation forces, the fluctuation-induced forces cannot always be separated into independent additive pair potentials. However, such a separation often works remarkably well.

[3] R. Holyst, D. J. Tweet, and L. B. Sorensen, Phys. Rev. Lett. **65**, 2153 (1990); D. J. Tweet, R. Holyst, B. D. Swanson, H. Stragier, and L. B. Sorensen, *ibid.* **65**, 2157 (1990).

[4] Tianming Zhang, Ph.D. thesis, University of Washington, 1994; Brian D. Swanson, Ph.D. thesis, University of Washington, 1993; Douglas J. Tweet, Ph.D. thesis, University of Washington, 1990.

[5] P. G. de Gennes, Langmuir **6**, 1448 (1990).

[6] B. D. Swanson, H. Stragier, D. J. Tweet, and L. B. Sorensen, Phys. Rev. Lett. **62**, 909 (1989).

[7] Brian D. Swanson, Ph.D. thesis, University of Washington, 1993.

[8] P. Richetti, P. Kekicheff, J. L. Parker, and B. W. Ninham, Nature (London) **346**, 252 (1990).

[9] A. J. Jin, T. Stoebe, and C. C. Huang, Phys. Rev. E **49**, R4792 (1994).

[10] The four liquid crystal materials we studied are 9O.4 [4-(*n*-nonyl)oxybenzylidene-4-(*n*-butyl)aniline], 4O.7 [4-(*n*-butyl) oxybenzylidene-4-(*n*-heptyl) aniline], 7O.7 [4-(*n*-heptyl) oxybenzylidene-4-(*n*-heptyl) aniline], and $\overline{14}$S5 [4-*n*-pentylbenzenethio-4-*n*-tetradecyloxybenzoate). The bulk phase transition temperatures (°C) for these materials are 9O.4 (Sm-*G* 67 Sm-*F* 69.5 Sm-*A* 82 *I*); 4O.7 (Sm-*B* 48.7 Sm-*C* 49.9 Sm-*A* 56.6 *N* 82.8 *I*); 70.7 (Sm-*G* 55 Sm-*B* 69 Sm-*C* 72.0 Sm-*A* 83.7 *N* 84 *I*); and $\overline{14}$S5 (Sm-*B*- 66.5 Sm-*A* 86.6 *I*).

[11] For reviews of surface freezing and surface melting, see J. G. Dash, in *Proceedings of the Nineteenth Solvay Conference,* edited by F. W. Dewitte (Springer-Verlag, New York, 1988); S. Dietrich, in *Phase Transitions and Critical Phenomena,* edited by C. Domb and J. Lebowitz (Academic, London, 1988), Vol. 12; M. Schick, in *Liquids at Interfaces,* edited by J. Charvolin, J. F. Joanny, and J. ZinnJustin (Elsevier, Amsterdam, 1990).

[12] Many different kinds of surface freezing and surface melting theories have been developed. For some examples, see (Landau theories) R. Lipowsky, Ferroelectrics **73**, 69 (1987); (density functional theories) R. Ohnesorge, H. Löwen, and H. Wagner, Phys. Rev. A **43**, 2870 (1991); (simple thermodynamic descriptions) J. K. Kristensen and R. M. J. Cotterill, Philos. Mag. **36**, 437 (1977); (lattice theories) A. Trayanov and E. Tosatti, Phys. Rev. B **38**, 6961 (1988). There has been one attempt to build a fluctuation based theory which predicts different behavior: R. Holyst, Phys. Rev. B **46**, 15 542 (1992).

[13] B. M. Ocko, A. Braslau, P. S. Pershan, J. Als-Nielsen, and M. Deutsch, Phys. Rev. Lett. **57**, 94 (1986). N.B., these authors did not interpret these measurements as arising from exponential forces, but their data follow the logarithmic growth law characteristic of exponential effective forces.